Radiation Damages Induced By Spallation Residues in ADS Window

C. Villagrasa, A. Boudard, J.-E. Ducret, B. Fernandez, S. Leray, C. Volant, P. Armbruster, T. Enqvist, F. Hammache, K. Helariutta, et al.

HAL Id: in2p3-00124227

http://hal.in2p3.fr/in2p3-00124227

Submitted on 12 Jan 2007

Radiation Damages Induced By Spallation Residues In ADS Windows

C. Villagrasa [1], A. Boudard [1], J.-E. Ducret [1], B. Fernandez [1], S. Leray [1], C. Volant [1],P. Armbruster [2], T. Enqvist [2], F. Hammache [2], K. Helariutta [2], B. Jurado [2], M.-V. Riccciardi [2], K.-H. Schmidt [2], K. Sümmerer [2], F. Vives [2], L. Audouin [3], L. Ferran [3], F. Rejmund [3], C. Stéphan [3], L. Tassan-Got [3], J. Benlliure [4], E. Casarejos [4], M. Fernandez [4], J. Pereira [4], S. Czájkowski [5], D. Karamanis [5], M. Pravikoff [5], J. George [6], R.A Mewaldt [6], N. Yanasak [6], M. Wiedenbeck[7], J. Connell [8], T. Faestermann [9], A. Heinz [10], A. Junghans [11]

1) DAPNIA/SPhN, CEA/Saclay, F-91191 Gif-sur-Yvette Cedex, France.
2) GSI, Planckstrasse 1, D-64291 Darmstadt, Germany
3) IPN Orsay, BP 1, F-91406 Orsay Cedex, France
4) University of Santiago de Compostela, 15706 Santiago de Compostela, Spain
5) CEN Bordeaux-Gradignan, F-33175, Gradignan, France
6) California Institute of Technology, Pasadena, CA 91125 USA
7) Jet Propulsion Laboratory,California Institute of Technology, Pasadena, CA 91109 USA
8) University of Chicago, Chicago, IL 60637, CA 91125 USA
9) TU Munich, 85747 Garching, Germany
10) Argonne National Laboratory, Argonne, IL 60439-4083 USA
11) CENPA/University of Washington, Seattle WA 98195 USA

Abstract-Isotopic distributions and recoil velocities of spallation residues produced in p+Fe reactions at several energies (300, 500, 750, 1000 and 1500 MeV) have been obtained recently using the reverse kinematics methods at GSI. The measured isotopic cross-sections allow calculating directly the chemical composition modifications expected in ADS windows after one year of operation while the recoil velocities can be used to assess the number of atom displacements (DPA). Results at different bombarding energies will be shown and compared to calculations performed with LAHET3, using standard models (actually the Bertini-Dresner combination) or the new INCL4-ABLA model (to be presented in this conference) recently implemented. Estimation of the contribution due to back-scattered particles from the target will be also discussed.

I. INTRODUCTION

The detailed design of Spallation Neutron Sources or Accelerator-Driven Systems (ADS) requires reliable computational tools in order to optimize their performance in terms of useful neutron production and to properly assess specific problems likely to happen in such systems. Among those problems are the radioactivity induced by spallation reactions, changes in the chemical composition and radiation damage in target, window or structure materials. Radiation damage can arise from gas production that causes embrittlement of structural materials and from atomic displacements (DPA) which fragilize the various components of the spallation source. Modifications of the chemical composition of these materials possibly result into problems of corrosion or alloy cohesion and modification of mechanical properties because of the appearance of compounds not existing initially in the materials.

Up to recently, only gamma-spectroscopy measurements of spallation residues with not too short and not too long half-lives or inclusive elemental cross-sections were available [1]. However, to determine the induced radioactivity and change in chemical composition, it is of prime interest to identify isotopically all the elements produced by spallation before radioactive decay. This can be realized only with the so-called reverse kinematics technique, which has been used in the last years at Saturne and at GSI for a wide range of nuclei at different energies. At GSI, the use of the FRagment Separator FRS allows to measure cross-sections down to the very light isotopes and to obtain recoil velocities of the fragments which are of great importance for DPA calculations. Radioactive decay calculations can then be applied to the measured isotopic cross-sections to determine the final chemical composition.

II. NEW EXPERIMENTAL DATA MEASURED AT GSI

The window between the proton accelerator and the spallation target preserves the vacuum existing in the accelerator and it is one of the most critical structure

materials in the ADS concepts. The proton beam traversing the window gives part of its energy by Coulomb interaction and creates residues by spallation reactions with a given recoil velocity that are going to change the chemical composition and create the atomic displacements in this material. The window is also hit by the back-scattered particles coming from the spallation target and the surrounding materials.

Several materials have been proposed for its composition as the martensitic steels T91 or EM10. These materials are formed at nearly 90 % by iron.

Historically the existing spallation data on iron [2-6] were measured for astrophysical purposes. Particularly only one set of data at one energy was available where the various residuals were isotopically identified [4]. These data were obtained at 573 MeV per nucleon and were limited to elements heavier than sulphur.

II.A. Experimental Set-up

Recently (October 2000) at GSI a larger set of data for iron residues was obtained using the magnetic spectrometer FRS (see Fig. 1.) facility in the framework of a programme to measure the residue cross sections down to 0.1 mb for a series of different projectile-target combinations and at different energies [7-10].

The experiment used the reverse kinematics: A beam of ^{56}Fe was extracted from the GSI heavy ion synchrotron (SIS) and directed onto a liquid hydrogen target [11]. All the fragments produced in the target were strongly forward focused and identified in flight.
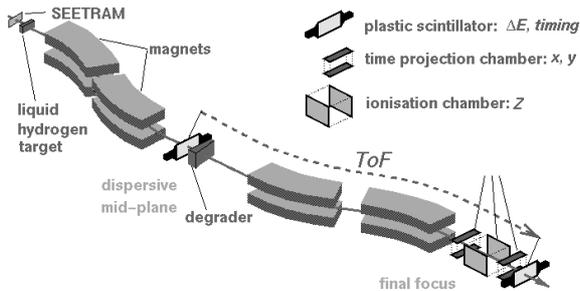

Fig. 1. Schematic layout of the FRS fragment spectrometer. The four large dipole magnets separate fragments. Scintillators measure the time of flight over the second half of the spectrometer as well as the horizontal fragment position. The MUSIC detector gives information about the energy loss by the fragment. Multi-wire chambers are used for beam tuning and removed for production measurements. The degrader was not necessary in this experiment.

The liquid-hydrogen target was enclosed between thin titanium foils of a total thickness of 36.3 mg/cm^2. The thickness of the liquid hydrogen was measured to be

87.3 ± 2.2 mg/cm^2. The ^{56}Fe beam was accelerated to energies of 0.3, 0.5, 0.75, 1.0 and 1.5 GeV per nucleon. Measurements were repeated in subsequent runs using an identical empty target to allow subtraction of contributions due to fragment production in the liquid target titanium windows.

The primary-beam intensity was continuously monitored and measured with the beam-current monitor SEETRAM from the current induced by secondary electrons in 3 Titanium thin foils.

Because of the FRS momentum acceptance (± 1.5 %), several measurements (settings) with various magnetic fields were done to cover all the momentum range of the fragments.

The mass-to-charge ratio, A/Z, of the fragments was determined from the magnetic rigidity using the relation (1)

$$\frac{A}{Z} = \frac{0.3 B\rho}{m_u \beta\gamma} \qquad (1)$$

where m_μ is the atomic mass unit, $B\rho$ the magnetic rigidity of the fragment and $\beta\gamma$ is related to the velocity of the fragment. The magnetic rigidity of the fragments, $B\rho$, is determined from positions at the focal planes measured with scintillators and the knowledge of the ion-optical conditions of the spectrometer. $\beta\gamma$ was experimentally measured from time of flight between the two focal planes (about 36 m of ToF base) where scintillators were placed.
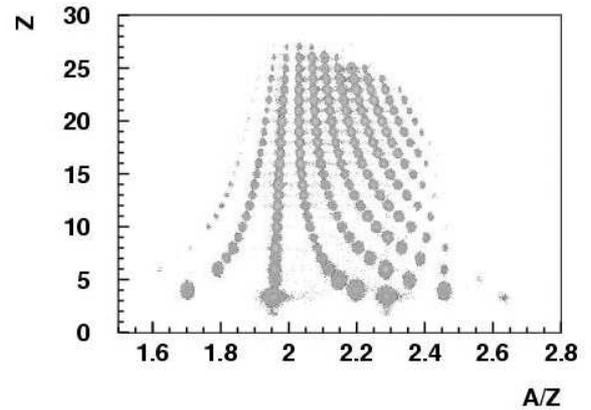

Fig. 2. Complete isotope coverage in Z vs. A/Z for 1 GeV/nucleon ^{56}Fe on an hydrogen target. The plot is made by superimposing data from overlapping magnet settings, normalized to the primary beam intensity.

The nuclear charge, Z, was determined using a multiple sampling ionization chamber (MUSIC) [12]. The energy loss in the gas produces a signal proportional to Z^2

β^2, allowing the determination of Z with a resolution of 0.15 charge units.

Fig. 2. shows the complete fragment coverage in Z versus A/Z for 1 GeV per nucleon ^{56}Fe on the hydrogen target. As it can be seen from this figure, all the residues were well identified down to very light fragments. The plot was made by adding data from individual settings, each normalized to the intensity of the primary beam.Once the identification of every fragment is done, the isotopic production cross section σ (Z,A) can be evaluated from N(Z,A), the number of detected ions, N_p the number of projectiles and N_t the number of target atoms per unit area. Several correction factors for systematic effects must be applied to these results which take into account the secondary reactions in the different layers of matter in the beam line, the contribution to the reaction rate from multiple reactions inside the hydrogen target, the detection efficiency and the FRS transmission factor. The latter is due to the limited geometrical acceptance (± 15 mrad) and the ion optical conditions of the FRS which result in a selection in the angular distribution of the fragments.

II.B. Results

In Fig. 3. current results of the mass distribution of the spallation residues on iron at five different energies are presented. All corrections mentioned in the section above have been made.

In Fig. 4. the isotopic distributions for fragments down to Na are presented for an energy of the projectile of 1.5 GeV. Experimental results are compared to the empirical parameterization EPAX [13] that is meant to describe the fragmentation of medium-to heavy-mass projectiles in the "limiting fragmentation" regime.
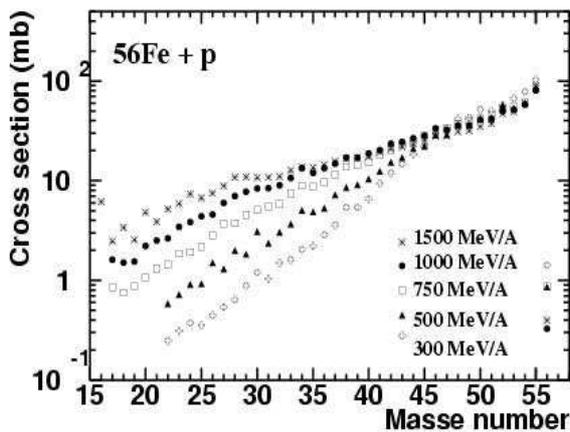

Fig. 3. Mass distribution of the fragments of the reaction Fe+p at different energies. Those are new data using the reverse kinematics method at GSI.

The position of the maximum of these isotopic curves depends on the transfer momentum in the collision between the projectile and the target. Nuclei close to the projectile are formed from very peripheral collisions. As the excitation energy is limited, only few particles may be evaporated by the pre-fragment, leading to the population of isotopes close to stability. For more central collisions, the excitation energy resulting in the pre-fragment is larger, and more neutron-deficient isotopes are produced.

The total uncertainty of the cross sections results from the combined errors on each correction factor and each quantity entering in the calculation of σ (Z,A). The total uncertainty of the cross sections is expected to be around 10%.
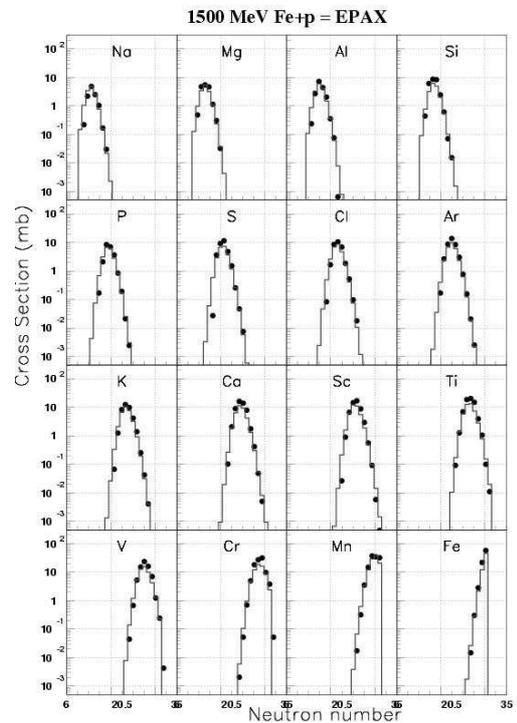

Fig. 4. Isotopic production cross section of fragments from the reaction Fe + p at 1.5 GeV/nucleon versus neutron number. These results are compare to the EPAX [13] parametric formula (continuous line).

In addition, the velocity spectrum of the fragments can also be obtained. The experimental time of flight between the intermediate and the final focal plane is precise enough for an accurate identification of the fragments. Nevertheless, due to a slight dependence on the trajectory it is not suited for a fine measurement of the velocity of the fragments. The velocity of the spallation residues in the laboratory frame was deduced from the magnetic rigidity in the first part of the spectrometer and the mass and charge number of the fragment.

Assuming that the reaction takes place in the center of the target, the fragment velocity is corrected for the energy loss in the target and transformed into the reference frame of the projectile. A measurement of the recoil velocity of the fragments is thus obtained. An example of velocity distribution for ^{28}Si residue produced in the reaction Fe +p at 1 GeV/A is displayed in Fig. 5. The kinetic energy of the fragments in the reference frame of the projectile is due to the momentum transfer between the target nucleus and the projectile and thus is a measurement of the violence of the collision. For each fragment, the distribution of the velocity component parallel to the beam is characterized by an average value and a width [14,15]. The width of the velocity distribution increases with the decreasing mass of the fragment.
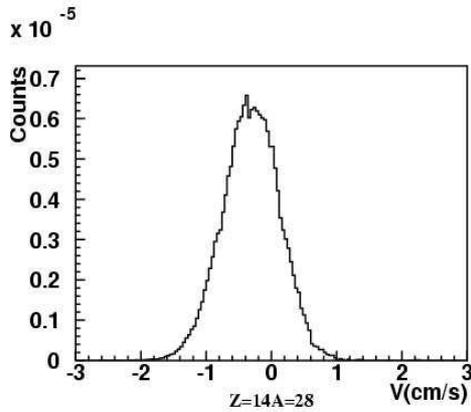

Fig. 5. Velocity spectrum in the beam rest frame of the projectile of ^{28}Si, one residue produced in the reaction Fe +p at 1 GeV/A. Negative values for the fragments means slower that the projectile

III. COMPARISON WITH CODES

Spallation reactions are generally described by a two-step mechanism: a first stage of individual nucleon-nucleon collisions, usually treated by an intranuclear cascade model (INC), then, the decay of the excited remnant nucleus by evaporation-fission.

In Fig. 6, comparison between the new experimental data and some of the existing models are presented. We show the charge distribution of the spallation residues on iron at 1 GeV/A compared to 3 different combinations of intranuclear cascade and evaporation codes.

These codes are represented by the curve: The upper picture shows the Bertini intranuclear cascade followed by the Dresner evaporation code [16,17] that are the default models used by LAHET3 [22]. In the center the INCL4 [20] intranuclear cascade and the GEM [23] evaporation-fission code is used. In the lower figure the

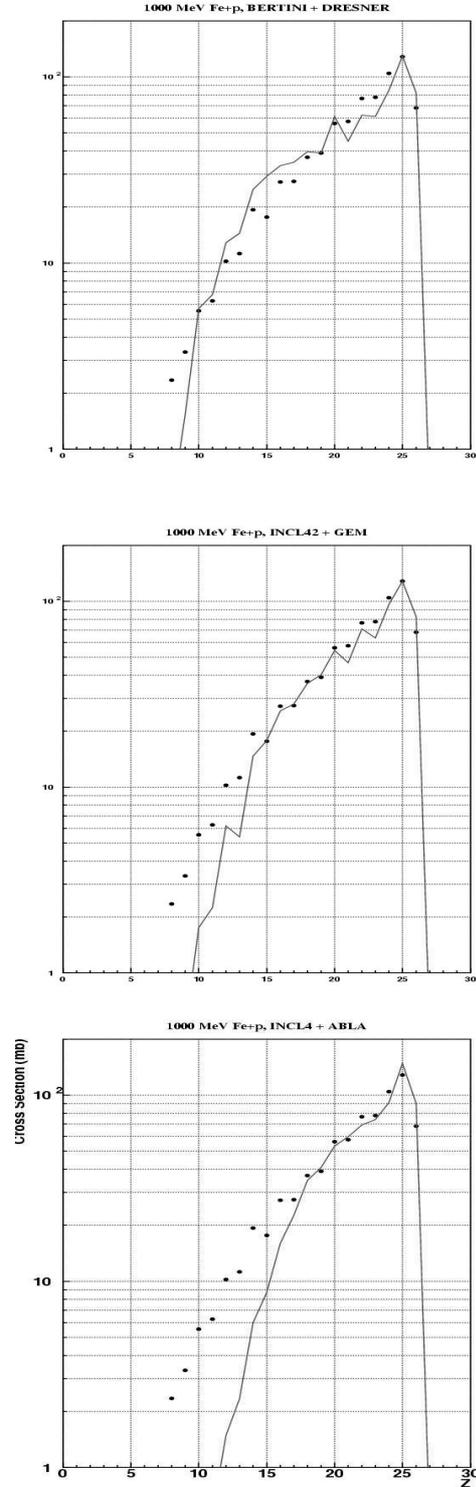INCL4 intranuclear cascade is followed by the ABLA [21] evaporation code.

Fig. 6. Comparison with code predictions (solid line) of the experimental charge distribution of spallation residues on iron at 1 GeV/A (dots) (See text).

The Bertini-Dresner combination gives a realistic total reaction cross-section (784 mb compared to the experimental one : 769 mb, at 1 GeV/A.) but it underestimates the heavier fragments and it overestimates the intermediate ones. This could suggest that the Bertini intranuclear cascade leaves too much excitation energy in the pre-fragment and so the number of evaporated particles increases leading to a major production of light fragments.

The behavior of the INCL4 intranuclear cascade is different. In general, the elements close to the projectile, which are responsible of the major part of the total reaction cross-section, are well reproduced. But the production of the lightest fragments is underestimated especially with ABLA. The main difference between the two evaporation codes shown in Fig. 6. is the even-odd effect in the production of the spallation residues that is better reproduced by the GEM evaporation code.

Concerning the fragments recoil velocities, the experimental data show a great discrepancy with those predicted by the codes as it can be seen from Fig. 7.
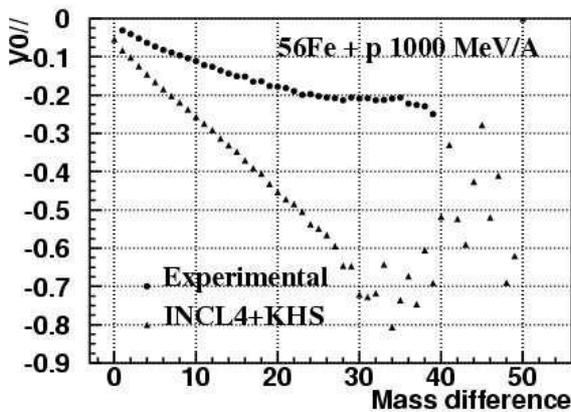

Fig. 7. Recoil velocity of the spallation residues at 1 GeV/A versus the mass difference between the mass of the projectile (56) and the residual mass. Solid dots : New experimental data at GSI. Empty squares : Values predicted by the INCL4 + ABLA codes.

The most interesting point in these data is that the recoil velocity does not increase linearly with the mass difference as it is predicted by the theory [14] and reproduced by the codes. Instead, the value of the recoil velocity seems to saturate at a value of the mass difference of twenty. This behavior is the same for the others energies analyzed in this experiment.

A possible explanation was given by P. Napolitani et al. [24]. Lightest fragments (not represented in the pictures above) would be mainly produced in a binary break-up of a heavy fragment ranging from ^{56}Fe to around ten mass units below, formed after the INC. The complementary fragment of this light fragment would be in the "saturated" region of the recoil velocity and both fragments would have the same recoil velocity, this of the pre-fragment.

These experimental data are of a great interest for the application in the calculation of the DPA for an ADS window. For this propose the recoil energy of the residues is used. The difference in the recoil energy between the codes and the experimental results is smaller than for the recoil velocities, so results are not very different (see section V)

IV. IMPURITY PRODUCTION RATE ON AN IRON WINDOW

Because the window of an ADS is thin enough to be considered as a thin target, an evaluation of the impurities produced in a steel window of an ADS system after one year of irradiation can be done directly from the experimental cross sections.

We have simulated an ADS window of 2 mm thickness composed by Iron along with a cylindrical Pb-Bi spallation target and surrounded by a heavy water moderator medium (See figure 8)
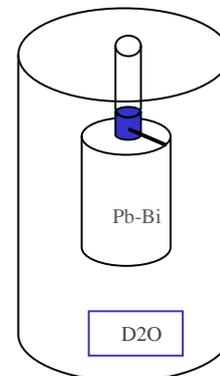

Fig. 8. Schematic representation of an ADS window followed by a Pb-Bi spallation target and surrounded by a heavy water medium.

The new experimental isotopic cross-section data were used to predict concentration of different elements, directly created by the proton beam on the window, after radioactive decay during one year of irradiation by a 31.8 µA/cm^2 proton beam at 1 GeV. The code ORIHET [26] was used to take into account the radioactive decay of

different isotopes during the irradiation time and the code DARWIN [25] estimate the contribution of thermal and epithermal neutrons activating the medium.

Final concentrations are given in appm (atoms of impurities in one million atoms of the target). They are plotted in Fig. 9. The full line represents the total concentration versus the element number after one year of irradiation.

Before this new experimental data, an evaluation of the concentrations created in a window was done using the models [18]. The difference with our data is important most of all for lightest elements as the models underestimate their production.

For fragility and embrittlement problems in the window material, special interest must be put in elements as phosphorus, calcium or sulfur created with important concentrations
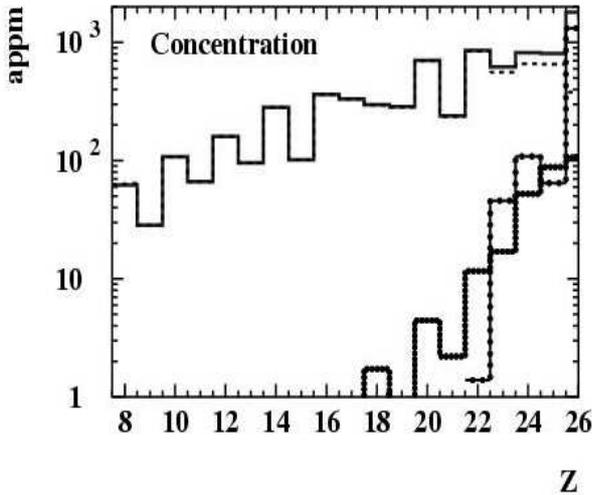

Fig. 9. Final concentrations versus element number in an ADS iron window after one year of irradiation by a 1 GeV proton beam of 31.8 µA/cm^2 current density. Full line: total concentration. Dashed line: concentration due to direct spallation of proton in the martensitic steel. Doted line: concentrations created in the window by light charge particles and neutrons of energies > 20 MeV coming from the surrounding medium. Dashed-doted line: products created in the window by neutrons with energies < 20 MeV in the medium.

V. DPA CALCULATIONS

Recoil velocities of the residues measured at GSI can be used in order to calculate the displacements per atom induced in the window.

We use a very simple method based in the equation of Robinson [27] and proposed in reference [19].

The total number of displacements produced by the residues created by spallation reactions in the window can be calculated as the addition of the displacements produced by each of this residues (Z,A)

$$D = \sum_{A,Z} \left(N_s \, \sigma(A,Z) \phi_t \right) d \left(E_d(A,Z) \right) \quad (2)$$

Where N_s is the surface target atoms, ϕ is the flux of incident protons, $\sigma(A,Z)$ the production cross-section of the residue (A,Z) (experimental result) and $d(E_d(A,Z))$ the number of displacements at an energy E_d.

Actually, all the recoil energy of the residue is not going to be useful to produce displacements because a part of it is lost by inelastic scattering with electrons in the medium. An estimation of the damage energy of the residue can be calculated using the Lindhard factor ξ [28]

$$E_d = E_r \cdot \xi \quad (3)$$

The number of displacements created by a residue (A,Z) are calculated using this damage energy and the Robinson formula :

$$d \left(E_d(A,Z) \right) = \frac{\eta \cdot E_d}{L} \quad (4)$$

where η = 0.8 and $L = 2E_b$ twice the energy binding an atom to its lattice site.

The total number of DPA created in the window by the same proton beam as the one described in section IV has been calculated using th experimental results of recoil velocities and production cross-sections of the residues. The result obtained by this method is **30 DPA/year** in the window. It can be compared with the **36 DPA/year** that one can find with the same DPA calculation method but with residual data obtained using the INCL4 + ABLA code.

A more accurate method can be used in order to calculated the DPA. The result that we have presented can be interpreted as an upper limit of the DPA produced after one year of irradiation.

VI. SUMMARY

An experiment using reverse kinematics for the reaction Fe + p took place at GSI using the FRS facility for different beam energies: 300, 500, 750, 1000 and 1500 MeV/A. New experimental data for isotopic cross

sections and recoil velocity for all these energies have been presented.

This new experiment provides a good identification and cross section measurements of all the spallation fragments coming out from the reaction down to Z=8.

Experimental recoil velocities of the fragments are especially surprising as they disagree with tendencies predicted by the theory and the codes. These experimental results together with the isotopic production cross-sections of the residues have been used in order to calculate the DPA created in the window after one year of irradiation. The calculations have been made using an analytic method. This result can be considered as un upper limit of the DPA produced. Differences between the result calculated from the experimental data and code data have been given.

In order to estimate the changes in the chemical composition induced by the proton radiation on an ADS window the experimental isotopic cross-sections at 1 GeV were used. An evaluation of the concentration of different fragments after one year of irradiation by a a 31.8 $\mu A/cm^2$ current density proton beam in a realistic ADS window have been presented.

Even though advices of metallurgy experts are needed to decide whether the created impurity concentrations are prohibitive, it can be seen from this calculations that some of the elements can create embrittlement problems in the window material as S with high concentrations (around 364 appm) or corrosion problems as Ca (around 700 appm).

REFERENCES

1.   R. MICHEL et al, *Nucl. Instr. and Meth. in Phys. Res.* **B103** 183 (1995).
2. W. R. WEBBER et al, *The Astrophysical Journal* **508** 949 (1998).
3.   W. R. WEBBER et al, *The Astrophysical Journal* **508** 940 (1998).
4.   W. R. WEBBER, J.C. KISH and D.A. SCHIER, *Phys. Rev.* **C41** 533 (1990). W.R. WEBBER, J.C. KISH and D.A. SCHIER, *Phys. Rev.* **C41** 547 (1990).
5. G.D. WESTFALL et al, *Phys. Rev.* **C19** 1309 (1979).
6. C. ZEITLIN et al, *Phys. Rev.* **C56** 388 (1997).
7. W. WlAZLO et al, *Phys. Rev. Lett.* **84** 5736 (2000).
8. T. ENQVIST et al *Nucl. Phys.* **A686** 481 (2001).
9. F. REJMUND et al, *Nucl. Phys.* **A683** 540 (2001).
10. J. BENLLIURE et al, *Nucl. Phys.* **A683** 513 (2001) .
11. P. CHESNY et al, *GSI Annu. Rep.* **97-1** 190 (1996).
12. PFÜTZNER et al, *Nucl.Instr. and Meth.* **B86**, 213 (1994)..
13. K. SÜMMERER and B. BLANK, *Phys. Rev.* **C61** *034607* 1 (2000).
14. A.S. GOLDHABER, *Phys. Lett.* **B53** 306 (1974).
15. D.J. MORRISSEY, *Phys. Rev.* **C39** 460 (1989).
16. H. W. BERTINI, *Phys. Rev.* **131** 1801 (1963).
17. L. DRESNER, *Oak Ridge report ORNL-TM-***196** (1962)
18. J. HENRY, C. VOLANT et R. LEGRAIN, *Note CEA/DAPNIA/SPhN-00-18 and CEA/NT/SRMA-00-2360*, (2000).
19. J. CUGNON C. VOLANT and S. VUILLIER, *Nucl. Phys.* **A620** 475 (1997).
20. A. BOUDARD , J. CUGNON, S. LERAY and C. VOLANT, *Phys. Rev.* **C66** *044615* (2002).
21. A. R. JUNGHANS et al, *Nucl. Phys.* **A629** 635 (1998).
22. R. E. PRAEL and H. LIECHTENSTEIN, *Los Alamos National Laboratory report LA-UR-89-3014*, (1989).
23. S. FURIHATA, *Proceedings of Monte Carlo 2000 Conference*, 23 Springer Verlag Lisbon, October (2000) ..
24. P. NAPOLITANI et al, *Proceeding of the XLII Int. winter meeting on Nucl. Phys.*, Bormio (2003).
25. A. TSILANIZARA et al, *J of Nucl. Sc. And Tech. Suppl.* **1**-845 (2000).
26. F. ATCHISON, *Paul Scherrer Institute report*, **98** 12 (1998).
27. M. ROBINSON, *J. of Nucl. Materials* **216** 1 (1994)
28.   M. LINDHARD, M. SCHARFF, *Phys. Rev.* **124** 128 (1961).